Int. J. Electrochem. Sci., 17 **(2022)** Article Number: 221138, doi: 10.20964/2022.11.44

International Journal of
ELECTROCHEMICAL
SCIENCE
www.electrochemsci.org

Electrochemical Sensors for Detection of Phenol in Oilfield Wastewater Using TiO_2/CNTs nanocomposite Modified Glassy Carbon Electrode

Wei Zheng[1], *ZhiGuo Zhou*[2], *Lan Wang*[3], *Yang Gao*[1], *ShiJun Chen*[4,*]

[1] No.6 Oil Production Plant of Changqing Oilfield Branch of PetroChina, Xi'an, Shanxi, 710000, Shaanxi Province, China
[2] No.12 Oil Production Plant Company of PetroChina Changqing Oilfield Company, Xi'an, Shanxi, 710000, Shaanxi Province, China
[3] No.7 Oil Production Plant Company of PetroChina Changqing Oilfield Company, Xi'an, Shanxi, 710000, Shaanxi Province, China
[4] College of Chemistry and Chemical Engineering, Xi'an SHIYOU University, Xi'an, 710065, Shaanxi Province, China
[*]E-mail: sxcsj001@sina.com

Received: 5 August 2022 / *Accepted:* 9 September 2022 / *Published:* 10 October 2022

This study focused on the straightforward fabrication of a TiO_2 and carbon nanotube nanocomposite utilizing the electrodeposition method on GCE (TiO_2/CNTs/GCE) as a sensitive and versatile electrochemical sensor for phenol determination in oilfield wastewater samples. The simultaneous electrodeposition of well-crystalline TiO_2 nanoparticles and CNTs on the electrode surface was successfully predicted by structural and morphological analyses. A linear range of 0 to 200 µM, a sensitivity of 0.04408µA/µM, and a detection limit of 0.005 µM were determined for TiO_2/CNTs/GCE after electrochemical studies using the DPV technique showed that the synergistic effects of the CNTs and TiO_2 nanoparticles improved the catalytic reactions for determining phenol and enhanced the sensitivity and specificity the phenol sensor. According to comparisons with recently reported phenol sensors, TiO_2/CNTs/GCE was a wide linear range phenol electrochemical sensor with an appropriate detection limit value. The TiO_2/CNTs/GCE phenol sensor was used to analyze the accuracy and applicability of the sensor by measuring the amount of phenol in actual samples made from oilfield wastewater. The results demonstrated appropriate recovery (more than 99.25%) and RSD values (less than 4.52%), which demonstrated the accuracy and viability of TiO_2/CNTs/GCE for phenol level assessment in oilfield wastewater samples. The results showed good agreement between the results from DPV measurements and Phenol Colorimetric Assay Kit assays.

Keywords: Electrodeposition; Nanocomposite; TiO_2 Nanoparticles; Carbon Nanotubes; Phenol; Oilfield Wastewater; Differential Pulse Voltammetry

1. INTRODUCTION

Wastewaters from oil-related sectors are generally referred to as oilfield and petrochemical wastewaters [1, 2]. Petrochemical wastewater can come from a variety of places, including oilfield production, refineries for crude oil, olefin processing factories, refrigeration, energy facilities, and other occasional wastewaters [3-5]. Wastewater from oil fields may be combined with oil at various concentrations. Fats, hydrocarbons, and petroleum fractions including kerosene, gasoline, and diesel oil can all be found in oil mixtures with water [6-8]. Many of those contaminants are harmful, and when they get into our water systems, they can have substantial short- and long-term health effects. Petrochemical waste is a complicated combination made up of several complex hydrocarbon molecules, including aliphatics, aromatics, asphaltenes, nitrogen-oxygen-sulfur, and phenolic compounds [9, 10].

The effluents of numerous sectors, including oil refining, petrochemicals, medicines, coking operations, resin manufacture, plastics, paint, pulp, paper, and wood products, contain phenolic compounds [11, 12]. The neurological system, eyes, nose, throat, skin, and eyes may get irritated after being exposed to phenol [13, 14]. Weight loss, sluggishness, weariness, soreness in the muscles, and weakness are a few signs of phenol exposure [15, 16]. Skin burns, tremors, convulsions, twitching, and liver and/or kidney damage can all result from severe exposure. Phenol is a protoplasmic toxin with a wide range of effects [17, 18]. It may easily penetrate cellular membranes thanks to its dual hydrophilic and lipophilic characteristics, denaturing proteins in the process and ultimately causing cell death and necrosis. Another possibility is a caustic impact that leads to coagulation necrosis. Respiratory irritation, headaches, and burning eyes can all be brought on by short-term exposure to phenol in the air [19, 20]. High phenol skin exposure leads to skin burns, liver damage, black urine, abnormal heartbeats, and even death in certain cases.

Some of the analytical methods investigated for determining phenol level include gas chromatography-mass spectrometry assay [21], high-performance liquid chromatography (HPLC) [22], electrochemical studies [23-25], spectrofluorimetric [26], spectroscopic [27] spectrophotometric and absorptiometric [28]. The utilization of expensive equipment and labor-intensive sample preparation are necessary for many of these approaches, though. Electrochemical investigations suggest low-cost, straightforward sample preparation, and highly sensitive phenolic compound identification methodologies among these methods [29-34]. Additionally, investigations showed that the selectivity and sensitivity of electrochemical sensors might be increased by adding nanostructures, composites, and nanohybrid materials to the electrode surface [35-37]. As a result, this study concentrated on the straightforward fabrication of TiO_2/CNT nanocomposite on GCE as a sensitive and versatile electrochemical sensor for phenol determination in samples of oilfield wastewater.

2. EXPERIMENT

2.1. Electrochemical modification of electrode

Before electrochemical modification, raw GCE was sequentially polished on a felt-polishing pad with 0.3 μm and 1 μm Al_2O_3 powders (Sigma-Aldrich), respectively. This was done after 10

minutes of ultrasonication in an ethanol and deionized water mixture. In a standard three-electrode electrochemical cell with a working electrode (GCE), counter electrode (Pt wire), and reference electrode (Ag/AgCl (3 M KCl)), electrodeposition was carried out using an electrochemical workstation potentiostat (CS350, Wuhan Corrtest Instruments Corp., Ltd., China) [38]. The electrolyte a solution of 3 M KCl (≥99.0%, Sigma-Aldrich) containing 8 mM H_2O_2 (30%, Sigma-Aldrich), 5 mg/L of CNTs (95%, Luoyang Advanced Material Co., Ltd., China) and 10 mM $Ti(SO_4)_2$ (≥70.0%, Sigma-Aldrich). Through CV electrochemical deposition at potentials between -0.15 and 0.15 V with a scanning rate of 10mV/s for 30 cycles, the TiO_2/CNTs composite was created on the surface of GCE. In order to electrodeposit pure CNTs on GCE, $Ti(SO_4)_2$ was not used in the electrolyte, and in order to electrodeposit pure TiO_2 on GCE, CNTs were not used in the electrolyte. Following electrochemical deposition, deionized water was used to rinse the modified electrodes before they were dried at room temperature.

2.2. Characterization instruments

Differential pulse voltammetry (DPV) measurements were performed using an electrochemical workstation potentiostat galvanostat (TOB-CS-150, Xiamen Tob New Energy Technology Co., Ltd., China). It was equipped with a three-electrode electrochemical cell that contained an Ag/AgCl reference electrode, a platinum plate counter electrode, and a bare or modified GCE (working electrode). All DPV measurements were carried out in a 0.1M phosphate buffer solution (PBS) electrolyte (pH 7.0) which was prepared from 0.1M NaH_2PO_4 (99%, Merck Millipore, Germany) and 0.1M Na_2HPO_4 (99%, Merck Millipore, Germany) in an equal volume ratio. Field emission scanning electron microscopy (SEM; Hitachi S-4800, Tokyo, Japan) and an X-ray diffractometer (XRD, Rigaku Miniflex 600, Rigaku, Tokyo, Japan) were used to evaluate the morphological and crystallographic properties of the nanostructures.

2.3. Preparation the real sample of oilfield wastewater

The TiO_2/CNTs/GCE phenol sensor was used to analyze the accuracy and applicability of the sensor by measuring the amount of phenol in actual samples made from oilfield wastewater. Samples of the oilfield wastewater were taken from the Songliao Plain's Daqing Oilfield's wastewater treatment facility in northeastern China. The collected wastewater samples underwent filtering and a ten-minute, 1200 rpm centrifugation process. The resulting supernatants were then utilized to make 0.1 M PBS (pH 7.0). For analytical experiments, standard addition was used. The actual samples were also examined using a Phenol Colorimetric Assay Kit from Elabscience Corporation.

3. RESULTS AND DISCUSSION

3.1. Structural and morphological studies of electrodeposited nanostructures

The modified GCE produced with electrodeposited CNTs, TiO_2, and TiO_2/CNTs nanostructures is shown in FE-SEM micrographs in Figure 1. Figure 1a's FE-SEM micrograph of the

CNTs/GCE surface reveals electrodeposited interconnecting tubular networks of CNTs with a 40 nm average diameter. The FE-SEM micrograph of TiO_2/GCE (Figure 1b) shows that the TiO_2 nanoparticles are generated as porous particles that are almost uniform in size and spherical in shape with a 35 nm average diameter. The modified GCE for the TiO_2/CNT nanocomposite in Figure 1c shows that the simultaneous electrodeposition of TiO_2 nanoparticles and CNTs on the electrode surface was successful. Additionally, TiO_2 nanoparticles are anchored to the surface and margins of CNTs, resulting in increased porosity, a large exposed surface area, a quick electron transport channel, and complete electrolyte impregnation [39-41].

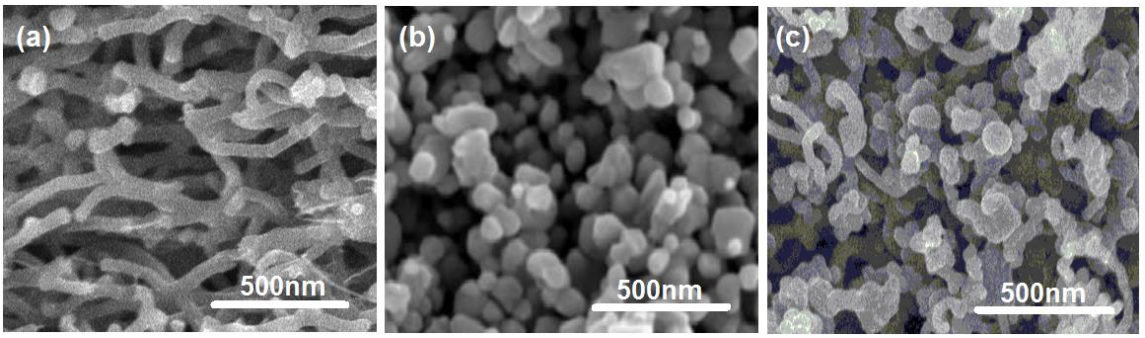

Figure 1. FE-SEM micrographs of modified GCE made with electrodeposited (a)CNTs, (b)TiO_2 and (c)TiO_2/CNTs nanostructures.

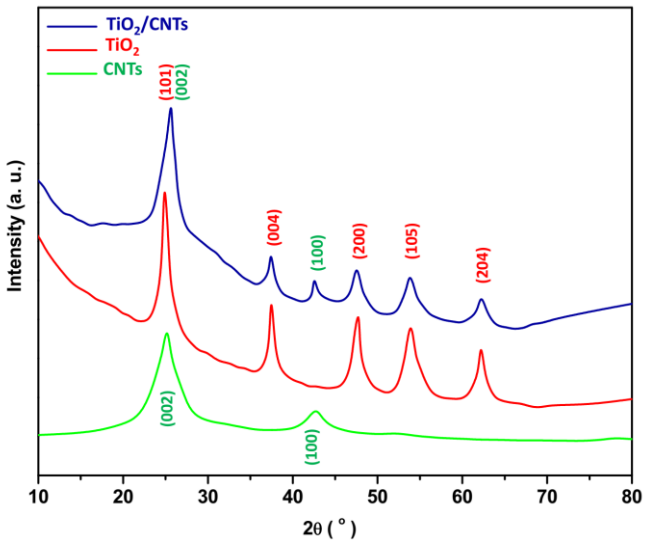

Figure 2. XRD pattern of structural characterization of powders of electrodeposited CNTs,TiO_2 andTiO_2/CNTs nanostructures.

The findings of the structural analysis of powders of electrodeposited CNTs, TiO2, and TiO2/CNT nanostructures are shown in Figure 2. The (002) and (100) Bragg reflection planes of the hexagonal structure of CNTs are ascribed to the characteristic diffraction peaks at 25.25° and 43.05° in the XRD pattern of CNTs (JCPDS card No. 75-1621) [42, 43]. There are diffraction peaks at 24.96°,

37.65°, 47.98°, 53.98°, and 62.46° that correspond to the (101), (004), (200), (105), and (204) crystalline planes of body-centered tetragonal TiO2 (JCPDS card No. 89-4921), as observed from the XRD profiles of TiO2 and TiO2/CNTs [44-46]. The presence of typical CNT diffraction peaks (002) and (100) in the XRD pattern of the TiO2/CNT nanocomposite indicates that it was successfully electrodeposited on the GCE.

3.2. Electrochemical studies

Figure 3 shows the DPV responses of the following materials: bare GCE,CNTs/GCE,TiO_2/GCE, and TiO_2/CNTs/GCE at the potential window of 0.00 V to 1.25 V with a scanning rate of 25 mV/s in 0.1 M PBS (pH 7.0) with and without 100 M phenol.

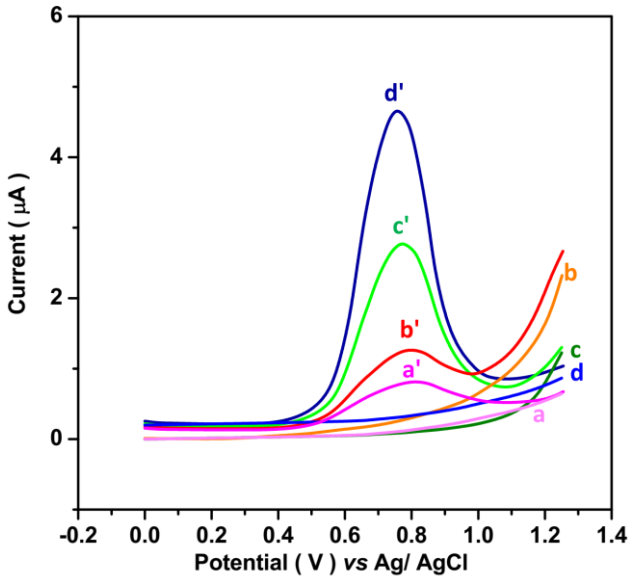

Figure 3. The DPV responses of (a and a') bare GCE, (b and b') TiO_2/GCE, (c and c') CNTs/GCE and (d and d') TiO_2/CNTs/GCE at the potential window from 0.00 V to 1.25 V with a scanning rate of 25 mV/s in 0.1 M PBS (pH 7.0) without and with 100 μM phenol.

As can be seen, all of the electrodes in the electrochemical cell do not exhibit a clear peak in the DPV curves when there is no phenol present. However, when there is 100 μM phenol present, the DPV curves of the GCE,TiO_2/GCE,CNTs/GCE, and TiO_2/CNTs/GCE show anodic peaks at 0.80 V, 0.79 V, 0.77 V, and 0.74V, respectively, which are attributed to the electrooxidation of phenol through the formation of the phenoxy radical [47, 48]. In contrast to TiO_2/CNTs/GCE, which show a typical peak current at a lower potential of 0.74 V that is around 3.7-fold and 1.7-fold greater than the peak currents of TiO_2/GCE and CNTs/GCE, respectively, a comparison of the DPV curves shows that the peak current of GCE is relatively weak at 0.80 V. According to research, TiO2 nanoparticles can successfully minimize the oxidation potential [49-51]. CNTs are advantageous materials for promoting the electrocatalytic capabilities of modified electrodes due to their significant electrical conductivity,

high porosity, large effective surface area, superior chemical stability, and mechanical strength [38, 52, 53]. According to FE-SEM images of the TiO_2/CNTs nanocomposite (Figure 1c), the TiO2 nanoparticles are highly dispersed on the surface of the CNTs, and the resulting morphology and interconnected nanoporous network can make it easier for electrons to move through the network during electrochemical reactions and thereby improve the TiO_2/CNTs nanostructures' electrochemical performance. The effective liquid-solid interfacial area is increased and more electrochemically active sites are provided on the surface of the nanocomposite when TiO_2 nanoparticles are concurrently anchored on a CNTs as a conductive support with high surface area [54-56]. For electrochemical experiments on the measurement of phenol, TiO_2/CNTs/GCE was employed for the synergistic effects of the CNTs and TiO2 nanoparticles in catalytic reactions for the determination of phenol.

The DPV reactions of TiO_2/CNTs/GCE in an electrochemical cell with 0.1 M PBS (pH 7.0) to injections of 10 µM phenol solutions at potentials ranging from 0.00 V to 1.25 V with a scanning rate of 25 mV/s are shown in Figure 4. With each injection of a 10 µM phenol solution into an electrochemical cell, the DPV peak current intensity at 0.74 V shows a noticeable increase. The calibration graph in Figure 4's inset shows that over the concentration range of 0 to 200 µM, the peak current intensity of DPV curves increases linearly, with an estimated sensitivity of 0.04408µA/µM and a determined detection limit of 0.005 µM. These data are summarized with recently reported phenol sensors in Table 1. The TiO_2/CNTs/GCE phenol electrochemical sensor has a large linear range and can be regarded as a novelty in the field [57]. Additionally, the functional groups and charged sites of the CNTs serve as numerous efficient active sites for the covalently attached TiO_2 nanoparticle catalysts, which increases the electrocatalytic activity. This work's TiO_2/CNTs/GCE also exhibits an adequate detection limit value [58-60]. Additionally, the High chemical and mechanical stability of the 1D structure of CNTs enables electron transfer from the electrode to the TiO_2 nanoparticles [52, 53, 61].

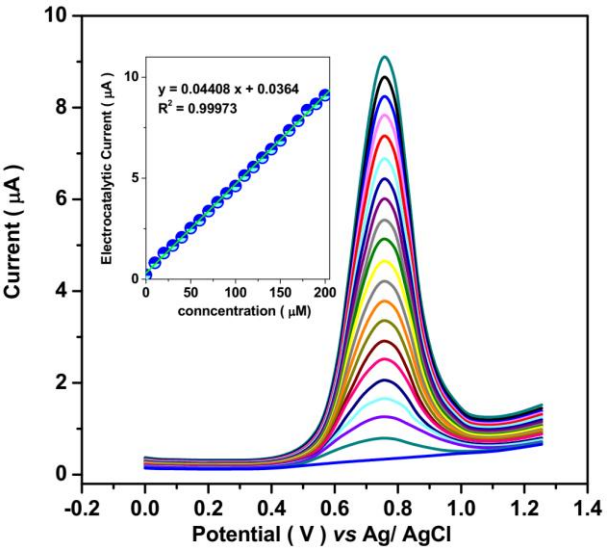

Figure 4. The DPV responses of TiO_2/CNTs/GCE toward injections of 10 µM phenol solutions at potentials ranging from 0.00 V to 1.25 V with a scanning rate of 25 mV/s in an electrochemical cell containing 0.1 M PBS (pH 7.0).

Table 1. Performance of phenol proposed sensing method in this work and other reported phenol sensor in literatures.

Electrode	**Technique**	**Detection limit (µM)**	**Linear range(µM)**	**Ref.**
GCE	DPV	0.5	0.5 to 5	[29]
Graphene nanosheet paste electrode	DPV	0.05	0.08 to 80	[30]
Polypyrrole/polyvinylpyrrolidone	CV	0.1	1 to 100	[31]
MWCNT/ dimethylditetradecylammonium bromide-tyrosinase/nafion/carbon paste electrode	CV	1.1	1.5 to 25	[33]
ZnO/screen printed electrode	LSV	0.004	0.01 to 50	[34]
Tyrosinase/MWCNTs/screen-printed electrode	Amperometry	1.35	2.5 to 75	[32]
TiO_2/CNTs/GCE	DPV	0.005	0 to 200	This work

CV: cyclic voltammetry; LSV: Linear sweep voltammetry

Under successive injections of various chemicals contained in oilfield wastewater, specificity of the TiO_2/CNTs/GCE as a phenol electrochemical sensor was examined. The results of the electrocatalytic signal of DPV measurement employing TiO_2/CNTs/GCE at potentials ranging from 0.00 V to 1.25 V with a scanning rate of 25 mV/s into 0.1M PBS under successive injections of 5 µM phenol solution and 30 µM of interfering chemicals are shown in Table 2. As can be seen, adding phenol solution to an electrochemical cell causes the generation of a noteworthy electrocatalytic signal, whereas adding interference-causing substances results in the absence of any observable electrocatalytic signal. Thus, it can be said that the suggested phenol sensor demonstrates a high degree of specificity for phenol measurement in samples of oilfield wastewater.

Table 2. The outcomes of electrocatalytic signal of DPV measurement using TiO_2/CNTs/GCE at potentials ranging from 0.00 V to 1.25 V with a scanning rate of 25 mV/s in 0.1 M PBS (pH 7.0) under sequential injections of 5 µM phenol solution and 30 µM of interfering compounds.

Substances	**Added(µM)**	**Electrocatalytic signal current (µA) at 0.74** V	**RSD**
Phenol	5	0.2206	±0.0041
α-naphthol	30	0.0267	±0.0018
Catechol	30	0.0611	±0.0019
p-chlorophenol	30	0.0231	±0.0014
Hydroxyphenol	30	0.0703	±0.0021
Hydroquinone	30	0.0408	±0.0019
p-nitrophenol	30	0.0301	±0.0011
Bisphenol	30	0.0634	±0.0013
Pyrocatechol	30	0.0555	±0.0021
2-aminophenol	30	0.0220	±0.0014
NH_4^+	30	0.0321	±0.0016

HCO_3^-	30	0.0343	±0.0014
Ca^{2+}	30	0.0205	±0.0014
Pb^{2+}	30	0.0198	±0.0010
NO_3^-	30	0.0418	±0.0022
Al^{3+}	30	0.0222	±0.0015
Mg^{2+}	30	0.0514	±0.0020
Br^-	30	0.0304	±0.0017
K^+	30	0.0228	±0.0012
Fe^{3+}	30	0.0252	±0.0016
SO_4^{2-}	30	0.0315	±0.0015
Cl^-	30	0.0441	±0.0017

The TiO_2/CNTs/GCE phenol sensor was used to analyze the accuracy and applicability of the sensor by measuring the amount of phenol in actual samples made from oilfield wastewater. Results from an electrochemical cell containing produced 0.1 M PBS (pH 7.0) from oilfield wastewater at potentials between 0.00 V and 1.25 V with a scanning rate of 25 mV/s for a DPV measurement. Table 3 lists the analytical outcomes using the conventional addition approach. The results demonstrate the accuracy and viability of TiO_2/CNTs/GCE for phenol level assessment in oilfield wastewater samples and show good agreement between the results from DPV measurements and Phenol Colorimetric Assay Kit assays. They also present appropriate recovery (more than 99.25%) and RSD values (less than 4.52%).

Table 3. The obtained analytical results using from DPV measurements and Phenol Colorimetric Assay Kit for determination phenol in prepared real samples from oilfield wastewater.

	DPV measurement			Phenol Colorimetric Assay Kit		
spiked (µM)	**detected (µM)**	**Recovery (%)**	**RSD (%)**	**detected (µM)**	**Recovery (%)**	**RSD (%)**
0.00	0.09	---	3.36	0.11	---	3.78
2.00	2.08	99.50	4.18	2.09	99.00	4.59
4.00	4.06	99.25	3.89	4.07	99.00	4.50
6.00	6.05	99.33	4.52	6.06	99.16	4.33

4. CONCLUSION

This study concentrated on the straightforward fabrication of a TiO_2/CNT nanocomposite on a GCE surface using the electrodeposition method as a sensitive and versatile electrochemical sensor for phenol detection in oilfield wastewater samples. According to structural analyses, the simultaneous electrodeposition of well-crystalline TiO_2 nanoparticles and CNTs on the electrode surface was successful. The catalytic reactions for phenol determination were improved thanks to the synergistic effects of the CNTs and TiO_2 nanoparticles, which also increased the sensitivity and specificity of the phenol sensor. The linear range of 0 to 200 µM, a sensitivity of 0.04408µA/µM, and a detection limit of 0.005 µM were determined for TiO_2/CNTs/GCE. The results were compared to those of recently

published phenol sensors, and they demonstrated that TiO_2/CNTs/GCE was a wide linear range phenol electrochemical sensor with a suitable detection limit value. This was due to the fact that the functional groups and charged sites of the CNTs act as numerous efficient active sites for the covalently anchored TiO_2 nanoparticle catalysts, which improves the electrocatalytic activity. The TiO_2/CNTs/GCE phenol sensor was used to analyze the accuracy and applicability of the sensor by measuring the amount of phenol in actual samples made from oilfield wastewater. The results showed that the results from the Phenol Colorimetric Assay Kit tests and DPV measurements were in good agreement, and they exhibited suitable recovery and RSD values that showed the accuracy and viability of TiO_2/CNTs/GCE for phenol level evaluation in oilfield wastewater samples.

References

1. C. Yu, X. Chen, N. Li, Y. Zhang, S. Li, J. Chen, L. Yao, K. Lin, Y. Lai and X. Deng, *Environmental Science and Pollution Research*, 29 (2022) 18423.
2. F. Chen, J. Ma, Y. Zhu, X. Li, H. Yu and Y. Sun, *Journal of Hazardous Materials*, 426 (2022) 128064.
3. X. Mo, X. Liu, J. Chen, S. Zhu, W. Xu, K. Tan, Q. Wang, Z. Lin and W. Liu, *Environmental Science: Nano*, 9 (2022) 1617.
4. D. Ge, H. Yuan, J. Xiao and N. Zhu, *Science of The Total Environment*, 679 (2019) 298.
5. J. Rouhi, C.R. Ooi, S. Mahmud and M.R. Mahmood, *Electronic Materials Letters*, 11 (2015) 957.
6. F. Ahmed and A. Fakhruddin, *International Journal of Environmental Sciences & Natural Resources*, 11 (2018) 1.
7. J. Dong, R. Deng, Z. Quanying, J. Cai, Y. Ding and M. Li, *Applied Radiation and Isotopes*, 178 (2021) 109939.
8. H. Karimi-Maleh, H. Beitollahi, P.S. Kumar, S. Tajik, P.M. Jahani, F. Karimi, C. Karaman, Y. Vasseghian, M. Baghayeri and J. Rouhi, *Food and Chemical Toxicology*, (2022) 112961.
9. E. Koshlaf and A.S. Ball, *AIMS microbiology*, 3 (2017) 25.
10. A.M. Khaksar, S. Nazif, A. Taebi and E. Shahghasemi, *Journal of photochemistry and photobiology A: chemistry*, 348 (2017) 161.
11. Y. Yang, H. Zhu, X. Xu, L. Bao, Y. Wang, H. Lin and C. Zheng, *Microporous and Mesoporous Materials*, 324 (2021) 111289.
12. Q. Guan, G. Zeng, J. Song, C. Liu, Z. Wang and S. Wu, *Journal of environmental management*, 293 (2021) 112961.
13. K.H. Kilburn, *Archives of Environmental Health: An International Journal*, 49 (1994) 37.
14. T. Li, D. Shang, S. Gao, B. Wang, H. Kong, G. Yang, W. Shu, P. Xu and G. Wei, *Biosensors*, 12 (2022) 314.
15. M. Yang, C. Li, Y. Zhang, D. Jia, X. Zhang, Y. Hou, R. Li and J. Wang, *International Journal of Machine Tools and Manufacture*, 122 (2017) 55.
16. H. Karimi-Maleh, C. Karaman, O. Karaman, F. Karimi, Y. Vasseghian, L. Fu, M. Baghayeri, J. Rouhi, P. Senthil Kumar and P.-L. Show, *Journal of Nanostructure in Chemistry*, (2022) 1.
17. Y. Wang, C. Li, Y. Zhang, M. Yang, B. Li, L. Dong and J. Wang, *International Journal of Precision Engineering and Manufacturing-Green Technology*, 5 (2018) 327.
18. J. Rouhi, C.R. Ooi, S. Mahmud and M.R. Mahmood, *Materials Letters*, 147 (2015) 34.
19. E. Romagnoli, T. Barboni, P.-A. Santoni and N. Chiaramonti, *Natural Hazards and Earth System Sciences*, 14 (2014) 1049.

20. M. Husairi, J. Rouhi, K. Alvin, Z. Atikah, M. Rusop and S. Abdullah, *Semiconductor Science and Technology*, 29 (2014) 075015.
21. H. Bagheri, A. Saber and S.R. Mousavi, *Journal of Chromatography A*, 1046 (2004) 27.
22. L. Zhao and H.K. Lee, *Journal of Chromatography A*, 931 (2001) 95.
23. V.K. Gupta, H. Karimi-Maleh and R. Sadegh, *Int. J. Electrochem. Sci*, 10 (2015) 303.
24. F. Caetano, E. Carneiro, D. Agustini, L. Figueiredo-Filho, C. Banks, M. Bergamini and L. Marcolino-Junior, *Biosensors and Bioelectronics*, 99 (2018) 382.
25. H. Beitollahi, S. Tajik and P. Biparva, *Measurement*, 56 (2014) 170.
26. R. Todeschini, D. Galvagni, J. Vılchez, M. Del Olmo and N. Navas, *TrAC Trends in Analytical Chemistry*, 18 (1999) 93.
27. E. Khatiwora, V.B. Adsul, M.M. Kulkarni, N. Deshpande and R. Kashalkar, *International Journal of ChemTech Research*, 2 (2010) 1698.
28. F. Ochynski, *Analyst*, 85 (1960) 278.
29. J. Mathiyarasu, J. Joseph, K. Phani and V. Yegnaraman, *Indian Journal of Chemical Technology*, 11 (2004) 797.
30. F.-T. Hu and S.-Q. Liu, *International Journal of Electrochemical Science*, 7 (2012) 11338.
31. Z. Chen and M. Hojo, *Bunseki Kagaku*, 56 (2007) 669.
32. M. Guix, B. Pérez-López, M. Sahin, M. Roldán, A. Ambrosi and A. Merkoçi, *Analyst*, 135 (2010) 1918.
33. S. Hashemnia, S. Khayatzadeh and M. Hashemnia, *Journal of Solid State Electrochemistry*, 16 (2012) 473.
34. J. Liu, H. Huang, S. Zhong, X. She and D. Yin, *International Journal of Electrochemical Science*, 11 (2016) 3921.
35. Z. Jiang, G. Li and M. Zhang, *International Journal of Electrochemical Science*, 12 (2017) 5157.
36. Z. Bo and T. Zhibo, *International Journal of Electrochemical Science*, 15 (2020) 6177.
37. Z. Said, S. Arora, S. Farooq, L.S. Sundar, C. Li and A. Allouhi, *Solar Energy Materials and Solar Cells*, 236 (2022) 111504.
38. L.C. Jiang and W.D. Zhang, *Electroanalysis: An International Journal Devoted to Fundamental and Practical Aspects of Electroanalysis*, 21 (2009) 988.
39. W. Gao, Y. Shi, Y. Zhang, L. Zuo, H. Lu, Y. Huang, W. Fan and T. Liu, *ACS Sustainable Chemistry & Engineering*, 4 (2016) 6313.
40. H. Karimi-Maleh, R. Darabi, M. Shabani-Nooshabadi, M. Baghayeri, F. Karimi, J. Rouhi, M. Alizadeh, O. Karaman, Y. Vasseghian and C. Karaman, *Food and Chemical Toxicology*, 162 (2022) 112907.
41. J. Rouhi, M. Alimanesh, R. Dalvand, C.R. Ooi, S. Mahmud and M.R. Mahmood, *Ceramics International*, 40 (2014) 11193.
42. H. He and C. Gao, *Molecules*, 15 (2010) 4679.
43. X. Wang, C. Li, Y. Zhang, H.M. Ali, S. Sharma, R. Li, M. Yang, Z. Said and X. Liu, *Tribology International*, 174 (2022) 107766.
44. Y. Xie, H. Qian, Y. Zhong, H. Guo and Y. Hu, *International Journal of Photoenergy*, 2012 (2012) 1.
45. T. Gao, C. Li, D. Jia, Y. Zhang, M. Yang, X. Wang, H. Cao, R. Li, H.M. Ali and X. Xu, *Journal of cleaner production*, 277 (2020) 123328.
46. N. Naderi, M. Hashim and J. Rouhi, *International Journal of Electrochemical Science*, 7 (2012) 8481.
47. H. Nady, M.M. El-Rabiei and G.M.A. El-Hafez, *Egyptian Journal of Petroleum*, 26 (2017) 669.
48. J. Zhang, C. Li, Y. Zhang, M. Yang, D. Jia, G. Liu, Y. Hou, R. Li, N. Zhang and Q. Wu, *Journal of cleaner production*, 193 (2018) 236.

49. E. Arkan, G. Paimard and K. Moradi, *Journal of Electroanalytical Chemistry*, 801 (2017) 480.
50. L. Tang, Y. Zhang, C. Li, Z. Zhou, X. Nie, Y. Chen, H. Cao, B. Liu, N. Zhang and Z. Said, *Chinese Journal of Mechanical Engineering*, 35 (2022) 1.
51. X. Cui, C. Li, Y. Zhang, Z. Said, S. Debnath, S. Sharma, H.M. Ali, M. Yang, T. Gao and R. Li, *Journal of Manufacturing Processes*, 80 (2022) 273.
52. G. Valenti, A. Boni, M. Melchionna, M. Cargnello, L. Nasi, G. Bertoni, R.J. Gorte, M. Marcaccio, S. Rapino, M. Bonchio, P. Fornasiero, M. Prato and F. Paolucci, *Nature Communications*, 7 (2016) 13549.
53. T. Gao, C. Li, Y. Wang, X. Liu, Q. An, H.N. Li, Y. Zhang, H. Cao, B. Liu and D. Wang, *Composite Structures*, 286 (2022) 115232.
54. B. Gao, G.Z. Chen and G.L. Puma, *Applied Catalysis B: Environmental*, 89 (2009) 503.
55. X. Wu, C. Li, Z. Zhou, X. Nie, Y. Chen, Y. Zhang, H. Cao, B. Liu, N. Zhang and Z. Said, *The International Journal of Advanced Manufacturing Technology*, 117 (2021) 2565.
56. D. Jia, Y. Zhang, C. Li, M. Yang, T. Gao, Z. Said and S. Sharma, *Tribology International*, 169 (2022) 107461.
57. J. Rouhi, S. Mahmud, S.D. Hutagalung, N. Naderi, S. Kakooei and M.J. Abdullah, *Semiconductor Science and Technology*, 27 (2012) 065001.
58. W. Yuan, S. Lu and Y. Xiang, *Rsc Advances*, 4 (2014) 46265.
59. Y. Wang, X. Wu, J. Liu, Z. Zhai, Z. Yang, J. Xia, S. Deng, X. Qu, H. Zhang and D. Wu, *Journal of Environmental Chemical Engineering*, 10 (2022) 107091.
60. B. Li, C. Li, Y. Zhang, Y. Wang, D. Jia and M. Yang, *Chinese Journal of Aeronautics*, 29 (2016) 1084.
61. H. Maleh, M. Alizadeh, F. Karimi, M. Baghayeri, L. Fu, J. Rouhi, C. Karaman, O. Karaman and R. Boukherroub, *Chemosphere*, (2021) 132928.